



SPACE-CHARGE EFFECTS ON BUNCH ROTATION

K.Y. Ng

*Fermi National Accelerator Laboratory**

P.O. Box 500, Batavia, IL 60510

(July, 2001)

Abstract

The longitudinal and transverse space-charge effects on bunch rotation in the longitudinal phase space designed to produce an intense short proton bunch are discussed. A criterion for bunch length broadening due to space-charge modification of the rf potential is given. As for the transverse effect, the incoherent space-charge tune shifts will lead to path length difference among the beam particles. However, the cumulative path length difference is found to be too small to affect the bunch rotation, provided that the chromaticities are corrected.

Based on a talk given at the FFAG 2000 Workshop
KEK, Tsukuba, October 11–13, 2000

*Operated by the Universities Research Association, Inc., under contract with the U.S. Department of Energy.

I INTRODUCTION

Intense proton bunches as short as 1 to 2 ns are necessary for the efficient production of pions and muons in order to (1) minimize the expensive cooling process of the muons and (2) to obtain a reasonable amount of polarization of μ^\pm in a muon collider and of ν_μ and $\bar{\nu}_\mu$ in a neutrino factory. This can be done by bunch rotation in the longitudinal phase space prior to the extraction of the proton bunches.

In this article, we want to investigate the longitudinal and transverse space-charge effects on the intense beam during the rotation.

II LONGITUDINAL EFFECT

An experiment was performed at the IUCF Cooler Ring to study the rotation of proton bunches [1] operating below transition. Some parameters of the experiment are listed in Table I.

Table I: Some parameters of the bunch compression experiment at IUCF.

Kinetic Energy	202.8	MeV
Circumference	86.825	m
Rf harmonic h	5	
Rf frequency	9.8316	MHz
Revolution frequency $\omega_0/(2\pi)$	1.9663	MHz
Slip factor η	-0.628	

The maximum rf voltage employed in the experiment was $V_{\text{rf}} = 1000$ V, which corresponds to a small-amplitude synchrotron tune of $\nu_s = 1.164 \times 10^{-3}$. It was lowered adiabatically to a minimum of ~ 5 V and raised suddenly back to 1000 V. The bunch would be compressed in $\sim \frac{1}{4}$ synchrotron oscillation. The minimum bunch length observed was about $\sigma_\tau = 3.8$ ns.

The equations of motion governing time advance τ of a beam particle and its fractional

momentum spread δ in the bunch rotation are

$$\tau_{n+1} = \tau_n + \frac{2\pi\eta}{\omega_0}\delta_n, \quad (2.1)$$

$$\delta_{n+1} = \delta_n + \frac{eV_{\text{rf}}}{\beta^2 E} \sin h\omega_0\tau_{n+1} + \frac{\Delta U_{\text{spch}}}{\beta^2 E}, \quad (2.2)$$

where n is the turn number, $\omega_0/(2\pi)$ is the revolution frequency, V_{rf} is the rf voltage, h is the rf harmonic, E is the total nominal particle energy, β is the particle velocity relative to the velocity of light, and e is the particle charge. The energy increase per turn due to the space-charge force is

$$\begin{aligned} \Delta U_{\text{spch}} &= -\frac{e^2}{\omega_0} \left| \frac{Z}{n} \right|_{\text{spch}} \frac{\partial \rho}{\partial \tau} \\ &= -\frac{e^2 N_b}{\sqrt{2\pi}\omega_0\sigma_\tau^2} \left| \frac{Z}{n} \right|_{\text{spch}} \frac{\tau}{\sigma_\tau} e^{-\tau^2/(2\sigma_\tau^2)}, \end{aligned} \quad (2.3)$$

where $[Z/n]_{\text{spch}}$ is the space-charge impedance per unit revolution harmonic. Because of the presence of electron cooling in the experiment, we have assumed a Gaussian distribution for the longitudinal bunch profile $\rho(\tau)$, with rms length σ_τ , which is normalized to the number of particles per bunch N_b when integrated over the time advance variable τ . Notice that $|\Delta U_{\text{spch}}|$ assumes a maximum at $\tau = \pm\sigma_\tau$.

It is clear that the synchrotron tune ν_s is reduced depending on the space-charge impedance and the gradient of the local longitudinal beam distribution, $|Z/n|_{\text{spch}}\partial\rho/\partial\tau$. Thus, each particle oscillates with a different ν_s . When the repulsive space-charge force is larger than the focusing rf force, the particle embarks on a hyperbolic trajectory and becomes unstable. But this instability may not be important because there is only $\sim \frac{1}{4}$ synchrotron oscillation during the whole bunch rotation, and the instability, if it occurs, is most severe near the end of the rotation when the bunch is shortest and the intensity gradient is highest.

Notice that the reduction of the synchrotron tune or motion along hyperbolic trajectories actually helps to reduce the nonlinearity of the rotation. This is because the reduction is largest for particles in the core of the bunch at the one sigma width where the intensity gradient is at a maximum. On the other hand, the particles near the separatrices are affected by space charge only minimally. This allows the tails of the bunch to catch up and

thus reduces the number of particles in the tails. However, when the space-charge force is large enough, the bunch width will increase as a result of the hyperbolic trajectories for the core particles.

In the experiment, bunch intensity was $N_b = 1 \times 10^9$ and $[Z/n]_{\text{spch}} \sim -j1500 \Omega$. Figures 1, 2, and 3 show the simulations with space charge impedance $|Z/n|_{\text{spch}} = 0, 1000, 5000, \text{ and } 10000 \Omega$. The bucket length was ~ 102 ns and 102 bins each of width 1 ns were used in the simulations where 160,000 macro-particles were tracked. There were insignificant differences when the the number of macro-particles was doubled.

It is important to point out that although the bunch appears to have broadened as the space-charge impedance increases from zero, the actual rms length is shortened instead according to Fig. 5. The main reason comes from the reduction of the synchrotron tune near the center of the bunch. This reduction, as stated earlier, compensates for the nonlinearity of the rf force which imparts slower synchrotron tunes for particles near the separatrices. As a result, the moment when the rotated bunch is shortest becomes delayed also. This reduces the number of particles near the separatrices or in the tails of the bunch. Figure 6 shows the situations of $|Z/n|_{\text{spch}} = 0, 2000, 4000, 7000, 10000, 15000, 20000, 25000 \Omega$ at the moment when the rms bunch length is shortest. We see that although the rotated bunch appears to have broadened when $|Z/n|_{\text{spch}} > 5000 \Omega$, the rms bunch length actually does not increase much until $|Z/n|_{\text{spch}} \gtrsim 15000 \Omega$. Closer investigation also reveals the hyperbolic trajectories, especially in the last two plots of Fig. 6, that are responsible for the width broadening of the bunch.

We believe that the effect of space-charge distortion of the rf waveform is governed by the ratio of the space-charge force to the rf force. From Fig. 5, it appears that in order to have a final compressed bunch length $\sigma_\tau \lesssim 3.85$ ns, the space-charge impedance per harmonic must be limited to $|Z/n|_{\text{spch}} \lesssim 15000 \Omega$. In other words, the ratio of the space-charge force to the rf force must be less than the critical value of

$$\left. \frac{\text{Sp-ch force}}{\text{Rf force}} \right|_{\text{critical}} = \frac{eN_b|Z/n|_{\text{spch}}}{\sqrt{2\pi}h\omega_0^2\sigma_\tau^3V_{\text{rf}}} \sim 22.0 . \quad (2.4)$$

where the shortest compressed value of $\sigma_\tau = 3.8$ ns, obtained in the simulation for the IUCF bunch, has been used. It is important to point out that the actual space-charge impedance of the IUCF Cooler is only $|Z/n|_{\text{spch}} \approx 1500 \Omega$. What we are saying is that, while a rms bunch length $\sigma_\tau = 3.85$ ns can be obtained in the absence of space charge,

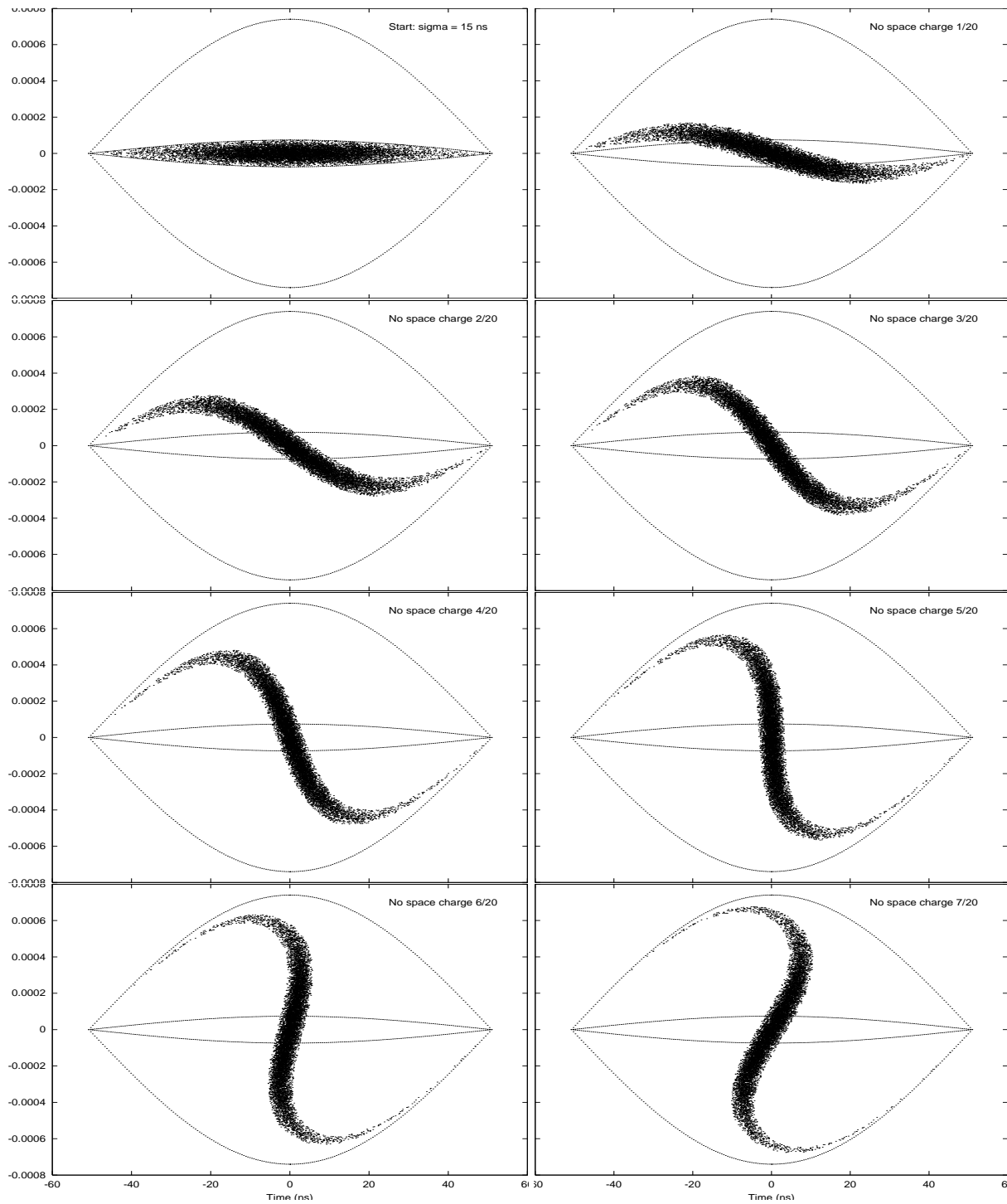


Figure 1: Phase-space plot of bunch rotation in the absence of space charge at start, $1/20$, $2/20$, \dots , $7/20$ of a synchrotron oscillation.

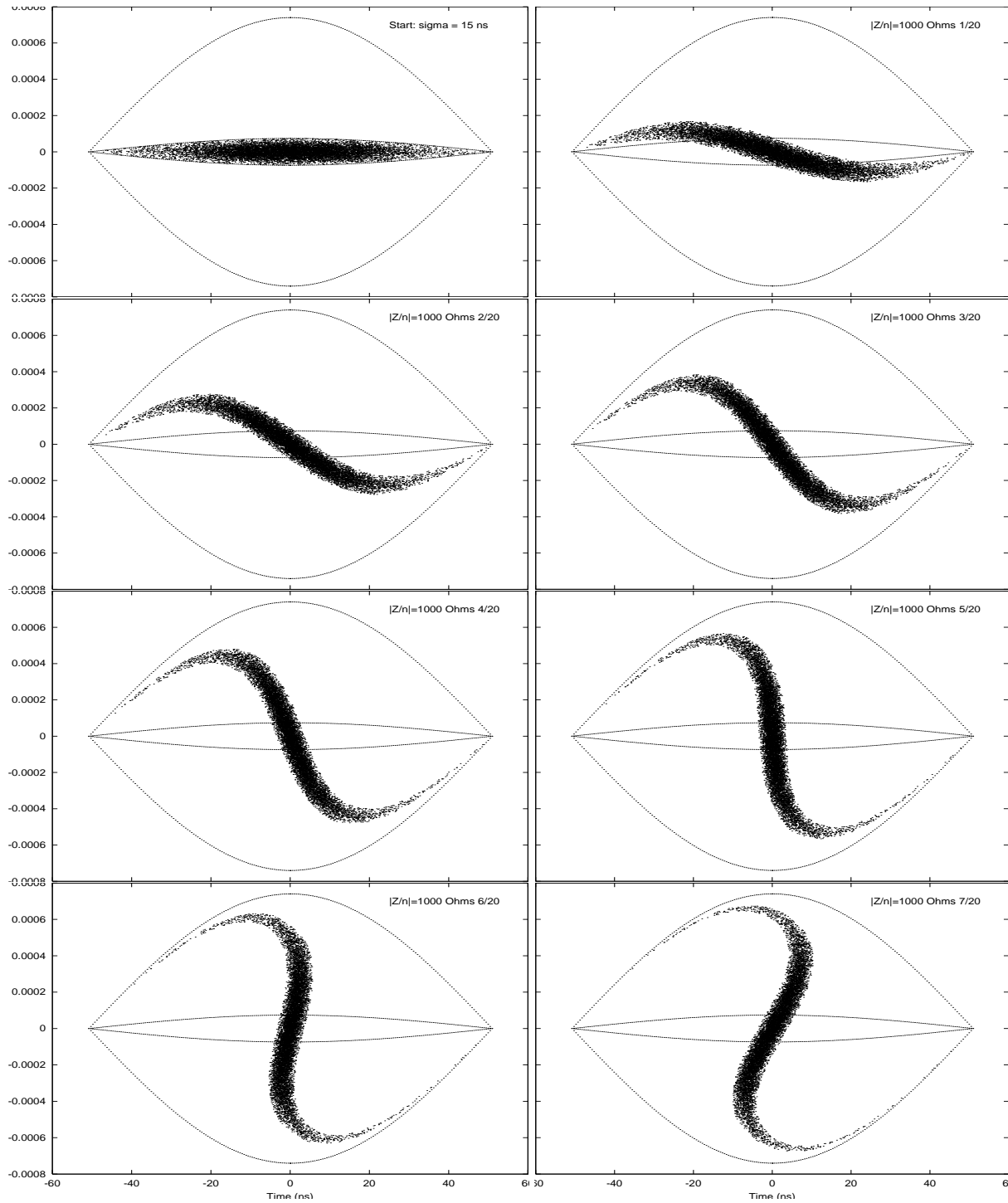


Figure 2: Phase-space plot of bunch rotation when $[Z/n]_{\text{spch}} = 1000 \Omega$ at start, $1/20$, $2/20$, \dots , $7/20$ of a synchrotron oscillation.

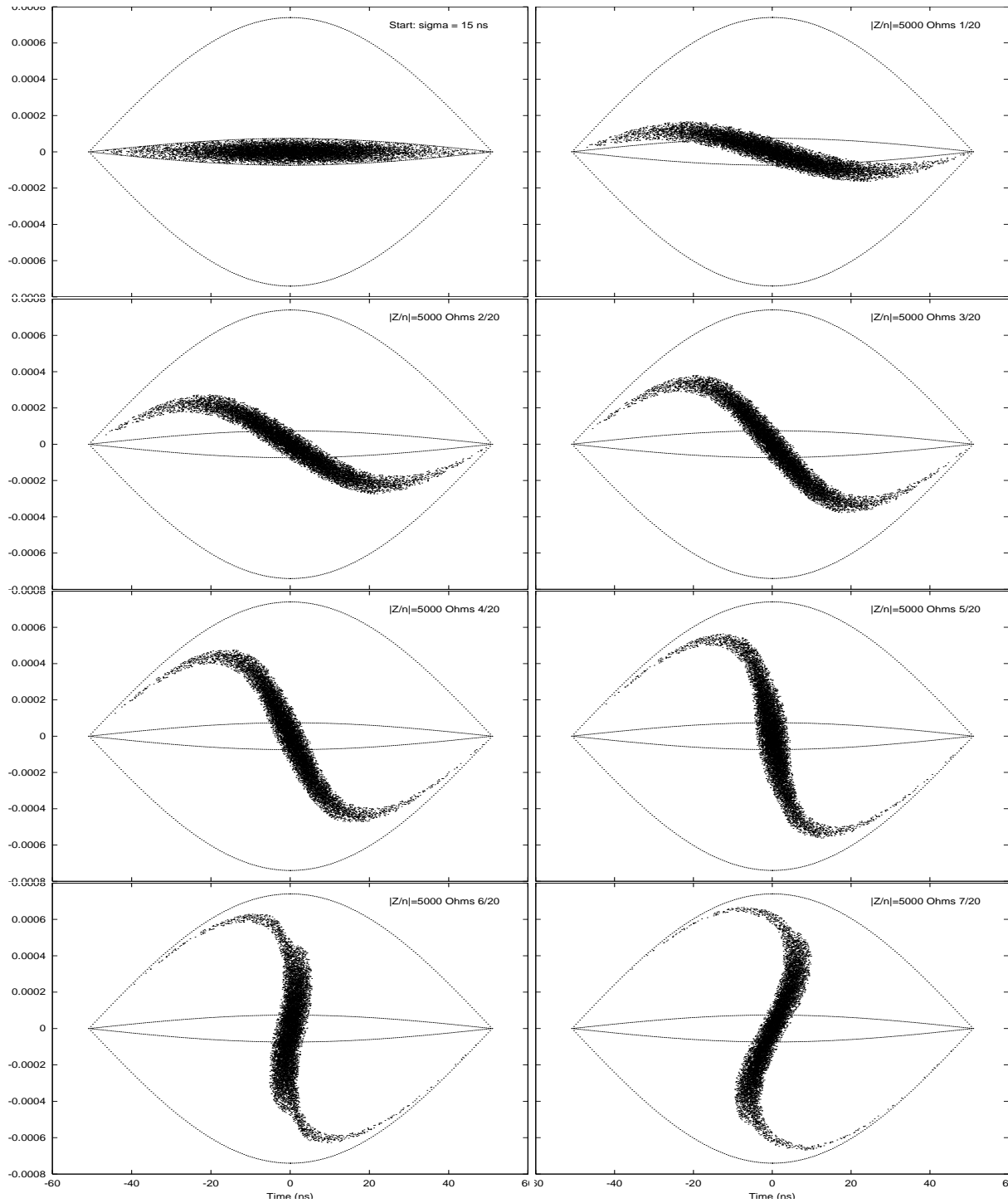


Figure 3: Phase-space plot of bunch rotation when $[Z/n]_{\text{spch}} = 5000 \Omega$ at start, $1/20, 2/20, \dots, 7/20$ of a synchrotron oscillation.

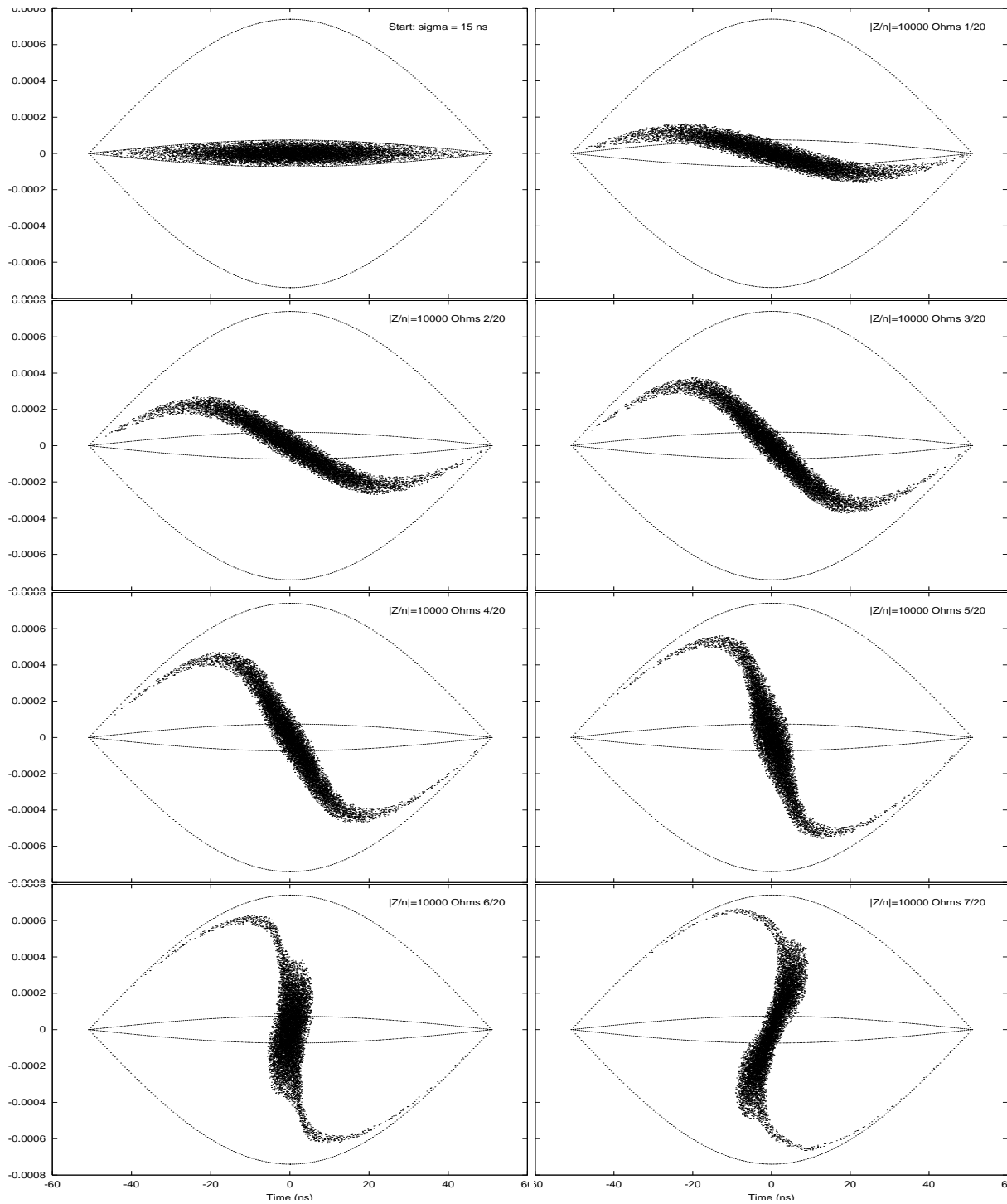


Figure 4: Phase-space plot of bunch rotation when $[Z/n]_{\text{spch}} = 10000 \Omega$ at start, $1/20$, $2/20$, \dots , $7/20$ of a synchrotron oscillation.

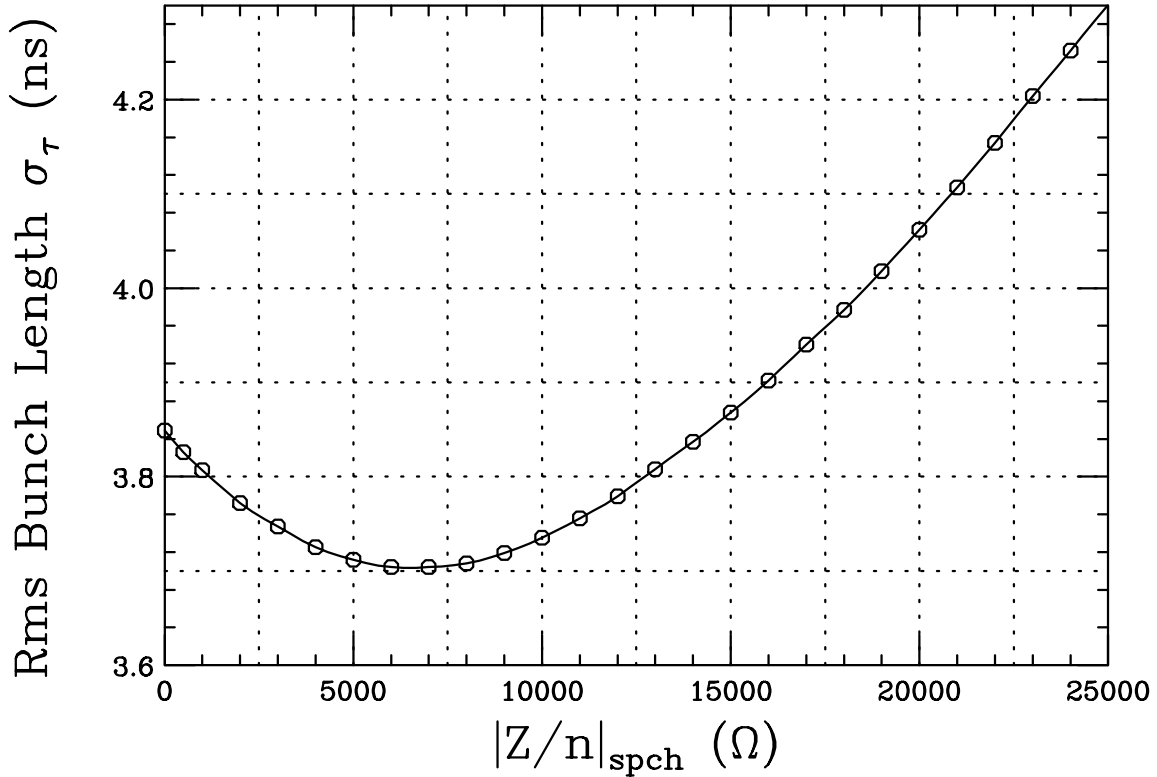


Figure 5: Plot showing shortest rms bunch length σ_τ obtained through rotation as a function of the space-charge impedance. When space charge is small, σ_τ becomes smaller as a result of reduction of synchrotron oscillation frequency near the core of the bunch. It increases rapidly later when space charge is large.

a space-charge impedance as large as $|Z/n|_{\text{spch}} \approx 15000 \Omega$ will not lead to a longer compressed rms bunch length although the rf potential will be severely distorted.

This ratio has been computed for Phase I (stage 2) and Phase II of the Fermilab Proton Driver. The results are listed in Table II. Notice that for Phase I of the Fermilab Proton Driver, the space-charge-to-rf ratio is very much less than the critical value of 22.0 stated in Eq. (2.4), implying that the bunch will not be affected significantly by the longitudinal space-charge force during bunch compression. For Phase II operation, the space-charge-to-rf ratio is roughly at the critical value. Thus, we expect that the longitudinal space-charge force will not broaden the bunch to more than the designed 1 ns during the bunch compression.

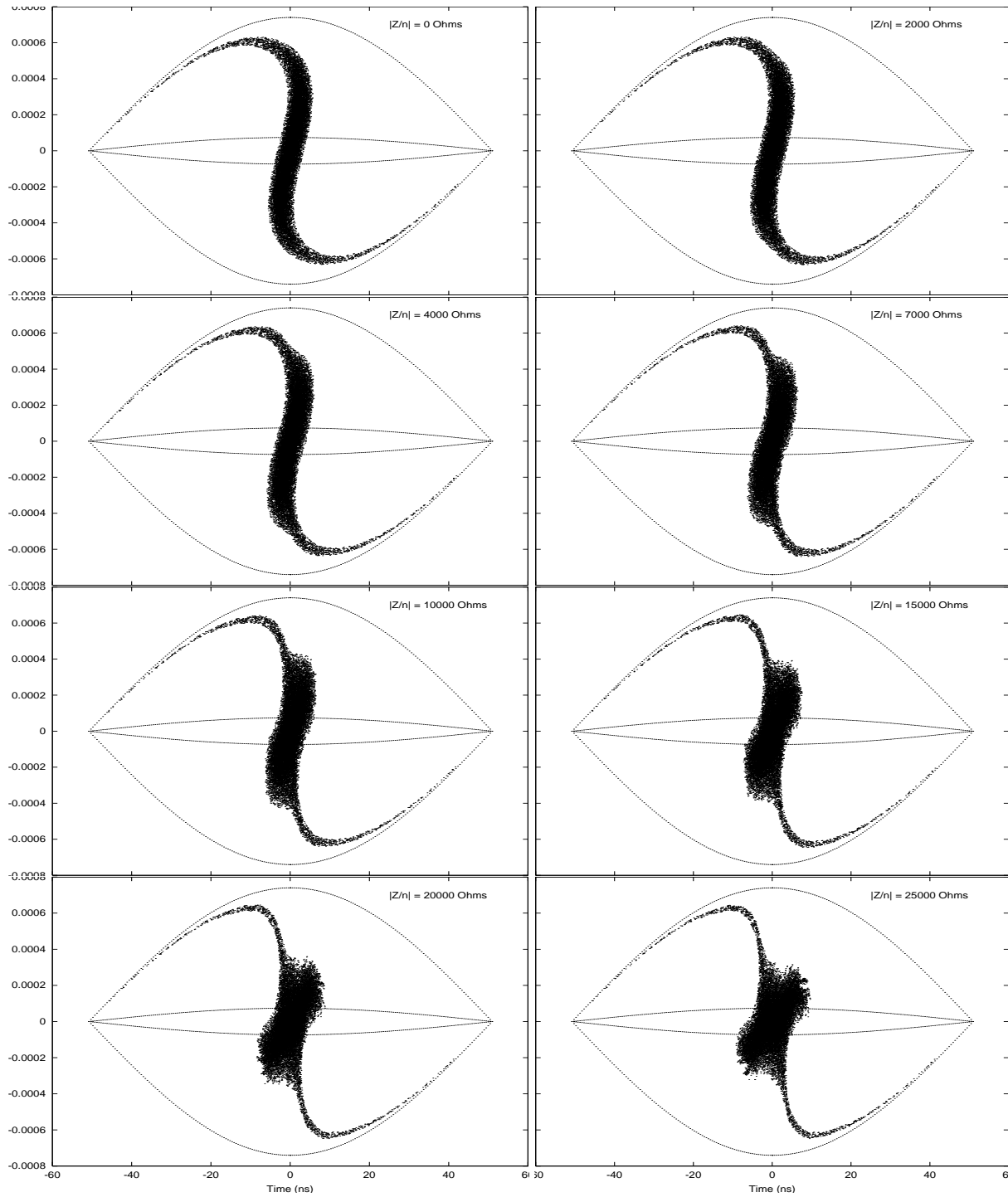


Figure 6: Phase-space plot of bunch rotation when the rms bunch length is shortest, where $[Z/n]_{\text{spch}}$ is assumed to be 0, 2000, 4000, 7000, 10000, 15000, 20000, 25000 Ω .

Table II: Comparison of the space-charge-to rf ratio in the experiment at the IUCF Cooler ring and bunch compression through rotation in Phase I and Phase II of the Fermilab Proton Driver.

	IUCF	Fermilab Proton Driver		
		Phase I	Phase II	
Circumference	86.825	711.32	711.32	m
Extraction kinetic energy	0.2028	16	16	GeV
Number per bunch N_b	$1 \cdot 10^9$	$1.7 \cdot 10^{12}$	$2.5 \cdot 10^{13}$	
γ	1.2161	18.053	18.053	
β	0.56909	0.99846	0.99846	
Revolution frequency	1.9650	0.42081	0.42081	MHz
g_0	4.468	4.560	4.560	
$ Z/n _{\text{spch}}$	15000	2.639	2.639	Ohms
V_{rf}	1.00	1400	1400	kV
Rf harmonic h	5	18	18	
Extraction σ_τ	3.85	3	1	ns
Sp-ch to rf ratio	22.0	0.060	23.9	

Some consideration is necessary if the bunch intensity in Phase II is increased. One way to ease the bunch compression problem is to go to a higher rf frequency. In the Phase II design, there will be a small lower-energy ring in between the linac and the 16-GeV Proton Driver. The lower-energy ring operates at the rf frequency of ~ 7.5 MHz. But the rf frequency of the 16-GeV ring can be doubled to ~ 15 MHz. This should be possible because in order to obtain a 1 ns-bunch at 16 GeV, the bunch area must be at least 3 times less than the bunch area designed for Phase I operation, otherwise the momentum aperture of the 16-GeV will not be large enough to hold the 1 ns-bunch.

Our consideration so far emphasizes on the effect of space-charge distortion of the rf potential. Microwave instability is less important during the rotation, because the local momentum spread increases. However, microwave instability can become a problem when the rf is lowered adiabatically to allow the bunch to fill the bucket. The simulations reported here have not taken this into account, because all the simulations start with the bunch matched to the bucket when the V_{rf} has been lowered.

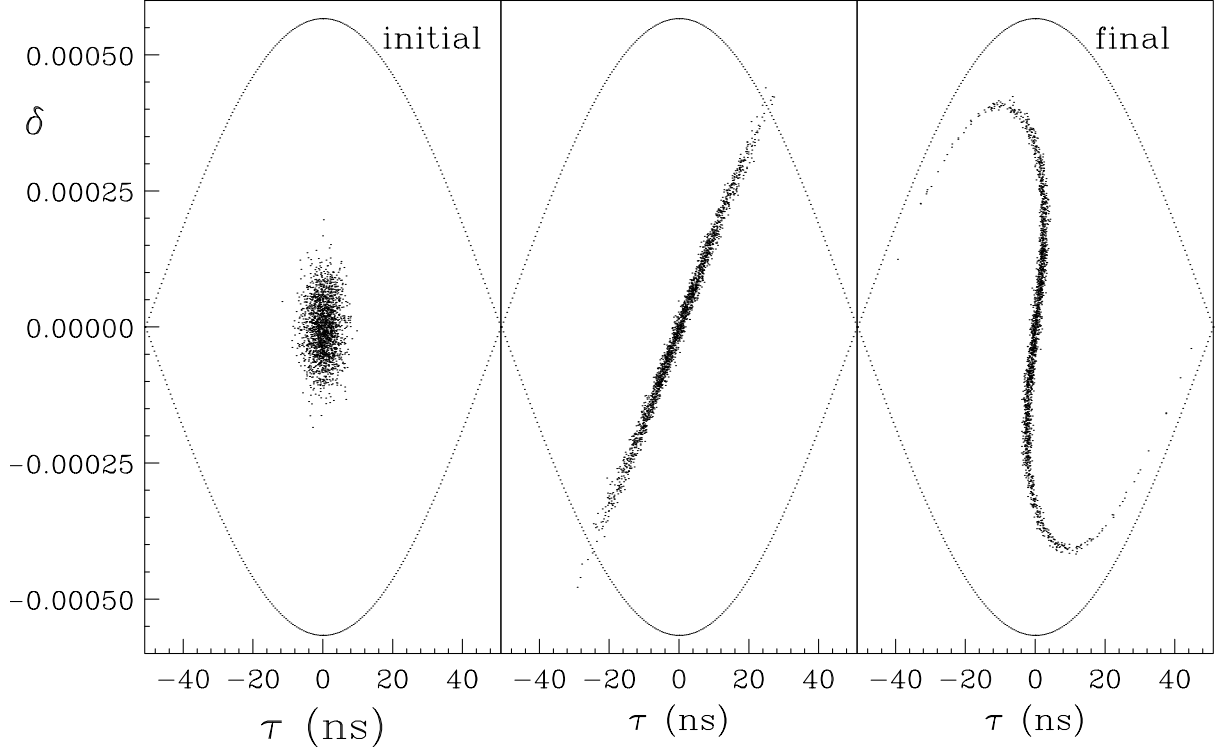


Figure 7: Evolution of bunch population through rf phase jump. Note that the particle motion is relatively linear near the unstable fixed point. Nonlinear rf potential becomes most important when the rf phase is shifted back to the stable fixed point.

To avoid microwave instability, it will be better not to compress the bunch by phase rotation. Instead, the method of synchronous phase jump should be used. The synchronous phase is jumped by π so that the bunch center is at an unstable fixed point in the longitudinal phase space. The bunch will lengthen along one set of separatrices and compress along the other set. After some time, the synchronous phase is jumped by $-\pi$ so that the bunch center is again at the stable fixed point. Allow for $\sim \frac{3}{8}$ of a synchrotron oscillation, the bunch will rotate to the situation of shortest length. This is illustrated in Fig. 7. The drift time along the separatrices cannot be too long. Otherwise, not all particles can return back to inside the bucket after the last phase switch. This allows us to derive the maximum possible compression ratio [1]

$$\frac{(\sigma_\tau)_f}{(\sigma_\tau)_i} \Big|_{\max} \sim \frac{\sqrt{2}}{\sqrt{3}(\sigma_\phi)_i}, \quad (2.5)$$

where $(\sigma_\phi)_i$ is the initial rms bunch length in rf radian.

One can also avoid the development of the nonlinear tails during the final rotation of $\sim \frac{3}{8}$ synchrotron oscillation. Instead of switching back to the stable fixed point, the bunch is extracted immediately at the end of the drift along the separatrices. The bunch is then sheared back to an upright position in the beam line via a lengthy optic system with local momentum compaction, or the R_{56} element of the transfer matrix.

Since this is not a rotation, the bunch length will be $\sqrt{2}$ longer than what was derived above. However, one may be able to recover this factor of $\sqrt{2}$ by allowing the bunch to drift somewhat longer along the separatrices before the extraction. This is possible because the bunch need not be recaptured into a bucket later.

III TRANSVERSE EFFECT

During bunch rotation, the bunch length is shortened and the incoherent space-charge tune shift increases. As an example, let us consider an earlier design of the Fermilab Proton Driver, which consists of a small ring of circumference 180.649 m accelerating protons from the kinetic energy of 1 GeV to 4.5 GeV. The rf harmonic is $h = 4$ and there are $n_b = 4$ bunches each with $N_b = 5.0 \times 10^{13}$ protons. The 95% normalized emittance is $\epsilon_{N95} = 200 \times 10^{-6} \pi\text{m}$. The incoherent space-charge tune shift at injection is

$$\Delta\nu_{sc} = -\frac{n_b N_b r_p}{2\gamma^2 \beta \epsilon_{N95} B_f} = -0.131, \quad (3.1)$$

where the bunching factor $B_f = 0.25$ has been used and a transverse uniform distribution has been assumed.

Bunch rotation is performed at the extraction kinetic energy of 4.5 GeV. When the rf voltage is reduced to its minimum, assume that the rms bunch length is $\sigma_\tau \sim \frac{1}{6}$ the bucket length. We would like to compress the bunch to $\sigma_\tau = 1$ ns by suddenly raising the rf voltage. The bunching factor B_f changes from 0.418 to 0.0164 during the bunch rotation. Correspondingly, the incoherent space-charge tune shift changes from $\Delta\nu_{sc} = -0.009$ to -0.225 , and different particles will have different betatron tunes, depending on their momentum offsets, betatron amplitudes, and local longitudinal densities. Reduction in betatron tune modifies the momentum compaction factor. Thus the path length of each

particle will be different and the bunch rotation in the longitudinal phase space will be affected. To the extreme, if the transition gamma is modified to such an extent that some particles find themselves above transition and some below transition, synchrotron rotation will be clockwise for some particles and counter-clockwise for some others. Also the higher orders momentum compaction may dominate over the zero order. Thus it is possible that the whole bunch compression through rotation would be jeopardized. In this section, we will analyze the effect of the space-charge tune shift and find out whether its influence to the bunch compression by rotation is damaging or not. This is a problem concerning the coupling between transverse motion and longitudinal motion. To investigate this problem, let us first revisit a similar problem in the muon collider ring.

III.1 REVISIT A SIMILAR PROBLEM

To maximize the luminosity, the first 2 TeV by 2 TeV muon collider design had low betatron functions of $\beta_x^* = \beta_y^* = 3$ mm at the interaction point [2]. The high betatron functions at the focusing triplets shoot up to ~ 400 km with natural chromaticities ~ -1500 . To avoid the hour-glass effect which will lead to luminosity reduction, the rms bunch length is chosen as $\sigma_\ell = 3$ mm. Short bunch length requires high rf frequency and therefore high rf voltage, making the rf system extremely expensive. As a result, one prefers to have the collider ring isochronous so that no rf system will be necessary.

At the Montauk Workshop in 1996, Bob Palmer [3] pointed out that particles entering the interaction point at a nonzero angle will have large-amplitude betatron oscillations and therefore longer path lengths. In the absence of synchrotron oscillation in an isochronous ring, the width of the bunch will be lengthened. Similar to the problem raised in the previous section, this is also a problem concerning coupling of transverse motion and longitudinal motion. It was found that [4] at the normalized emittance $\epsilon_N = 50 \times 10^{-6} \pi$ m, the path length reduction per turn can be as much as $\Delta\ell \sim 3.52 \times 10^{-5}$ m. In 1000 turns, the bunch would be lengthened by $\Delta\ell \sim 3.52$ cm. Note that the design bunch length is only $\sigma_\ell = 3$ mm.

To preserve the bunch length, one requires an exchange between head and tail through synchrotron oscillation or the collider ring cannot be isochronous. A rule of thumb is that during half a synchrotron period, the amount lengthened must be less than the rms bunch

length. Thus, for a designed rms bunch length of 3 mm, the synchrotron period has to be less than 170 turns. For a 150-turn synchrotron period, one would require a rf voltage of $V_{\text{rf}} = 1.5$ GV and a slip factor of $|\eta| \sim 1.5 \times 10^{-5}$ for the collider ring [3].

A few months later, Bob Palmer said that he was wrong. He learned from Oide that the large-amplitude path length would not be longer at least up to second order in betatron amplitudes, providing that chromaticities were corrected [5]. Étienne Forest gave a very general proof which explain the problem clearly [6].

Here, we are talking about path length per revolution, which is not a well-defined quantity, since the betatron tunes are not integers. A better defined quantity is the path length averaged over many revolutions. This definition is valid as long as one is not in a chaotic region in phase space.

When we average over many turns, the path length (which will always mean the averaged path length from now on) is dependent on J_x and J_y , the two betatron actions in the transverse planes, and cannot depend independently on the horizontal displacement x , horizontal momentum p_x , vertical displacement y , or the vertical momentum p_y . Note that J_x and J_y are invariants. The path length will also be a function of the momentum of the particle, which is constant in a storage ring without rf. Here, we denote it by δ , the fractional offset from the nominal momentum.

Proof of Theorem

The canonical variables are (a_x, J_x) , (a_y, J_y) , and $(-\Delta\ell, \delta)$. Here a_x and a_y are the angle variables conjugate to J_x and J_y in the two transverse planes. $\Delta\ell$ is the path length in excess of the length of the design closed orbit, or the length of the on-momentum orbit when the amplitudes of betatron oscillation are infinitesimal (see Appendix A). Note that $\Delta\ell$ is the actual path length difference instead of an advance along the on-momentum orbit. This is because the fractional momentum offset δ is measured with respect to the *total* nominal momentum p_0 and *not* the longitudinal momentum p_s .

Let us consider first an isochronous storage ring without rf so that the momentum offset δ is also a constant of motion. We also neglect self-field at this moment. Then, it is clear that the Hamiltonian will be cyclic in a_x , a_y , and $\Delta\ell$. If we expand it about the

design orbit, up to second order,

$$H = \nu_{0x}J_x + \nu_{0y}J_y + aJ_x^2 + 2bJ_xJ_y + cJ_y^2 + d\delta^2 + fJ_x\delta + gJ_y\delta . \quad (3.2)$$

Notice that the term proportional to δ is absent because comparison is made with respect to the on-momentum orbit with zero betatron amplitudes. From the equations of motion, we get the betatron tunes ν_x and ν_y ,

$$\nu_x = \left\langle \frac{da_x}{d\theta} \right\rangle = \frac{\partial H}{\partial J_x} = \nu_{0x} + 2aJ_x + 2bJ_y + f\delta , \quad (3.3)$$

$$\nu_y = \left\langle \frac{da_y}{d\theta} \right\rangle = \frac{\partial H}{\partial J_y} = \nu_{0y} + 2bJ_x + 2cJ_y + g\delta , \quad (3.4)$$

and the path length difference per turn $\Delta\ell_0$,

$$-\frac{\Delta\ell_0}{2\pi} = \left\langle -\frac{d\Delta\ell}{d\theta} \right\rangle = \frac{\partial H}{\partial \delta} = 2d\delta + fJ_x + gJ_y , \quad (3.5)$$

where $\langle \rangle$ denotes the average over one turn. The independent variable has been chosen as θ which increases by 2π per turn. We can readily identify a , b , and c as amplitude-dependent detunings, $d = -\frac{1}{2}\alpha_0 R$ with α_0 the momentum compaction factor, and f and g as the chromaticities. Thus, correcting the chromaticities will alleviate the dependence of path length on betatron amplitudes. The theorem can be extended by adding more higher-order terms to the Hamiltonian, and some higher-order chromaticity terms will enter into the right side of Eq. (3.5). These higher-order chromaticities must also be compensated, although extremely difficult in reality, in order that the path length difference due to betatron amplitudes will vanish to higher orders. We will go deeper into the compensation of path length in Appendices B and C.

It is because of this consideration that all lattices for the muon collider ring designed later can be made as close to isochronicity as one desires.

III.2 INCOHERENT TUNE SHIFT

Now let us add rf cavities. If the Proton Driver is dispersion-free at the cavities, the additional term in the Hamiltonian will not be dependent on the momentum deviation δ , and therefore Eq. (3.5) will not be affected, even though this additional term in the Hamiltonian depends on the betatron oscillation amplitudes, J_x and J_y .

We next include the self-field, which can be regarded as an external force acting on the particle under consideration. Notice that the self-field space-charge tune shift in Eq. (3.1) is inversely proportional to $\gamma^3\beta^2$ (since $\epsilon_{N95} \propto \gamma\beta$). Thus, the tune shift is momentum dependent and can be written as, with $z = x, y$,

$$\Delta\nu_z \approx \Delta\nu_{sc,z} (1 - 3\delta + 12\delta^2) , \quad (3.6)$$

where $\Delta\nu_{sc,z}$ is evaluated at the nominal momentum and is in general a function of betatron amplitudes. It is evident that the last two terms represent the first two lowest orders of chromaticity generated by the transverse space-charge force. Notice that the betatron action J_z is related to the transverse offset z from the off-momentum closed orbit by $z = \sqrt{2\beta_z J_z}$, where β_z is the betatron function. Thus, the contribution of the self-field space-charge tune shift to the Hamiltonian is

$$\Delta H = \Delta N_{sc}(J_x, J_y) (1 - 3\delta + 12\delta^2) - \frac{1}{2}R [\Delta\alpha_{sc,0} + \mathcal{O}(\delta)] \delta^2 , \quad (3.7)$$

where

$$\frac{\partial}{\partial J_x} \Delta N_{sc}(J_x, J_y) = \Delta\nu_{sc,x} \quad \frac{\partial}{\partial J_y} \Delta N_{sc}(J_x, J_y) = \Delta\nu_{sc,y} . \quad (3.8)$$

The second term[†] in Eq. (3.7) accounts for the change in momentum compaction factor arising from the space-charge tune shift. The dependency of $\Delta\alpha_{sc,0}$ on $\Delta\nu_{sc,x}$ is called Umstätter effect. For the situation of a uniform focusing ring, the lowest order momentum compaction factor is

$$\alpha_0 = \frac{1}{\nu_x^2} , \quad (3.9)$$

where ν_x is the horizontal tune. Thus, the space-space tune shift leads to a change of transition gamma

$$\Delta\gamma_t = \Delta\nu_{sc,x} . \quad (3.10)$$

Obviously, this relation will be lattice dependent and will be much more complicated in a realistic accelerator ring. In general $\Delta\alpha_{sc,0} + \mathcal{O}(\delta)$ is a function of momentum spread δ . Thus the derivative with respect to δ will give the extra fractional change in orbit length and therefore the change in all orders of the momentum compaction factor. However, $\Delta\alpha_{sc,0} + \mathcal{O}(\delta)$ must be J_x and J_y independent. This is because if it depends on J_x and

[†]This term has been mistakenly left out in Chapter 4 (p. 4-8) of *The Proton Driver Design Study*, Ed. W. Chou and C. Ankenbrandt, Fermilab Report TM-2136, 2000.

J_y , this term will contribute to the betatron tunes and thus modify the space-charge tune shifts $\Delta\nu_{sc,z}$ which we introduced earlier[‡]. This conclusion is extremely important since this second term in Eq. (3.7) will lead to the same shift in the transition gamma for all particles with the same momentum and at location with the same longitudinal density regardless of their transverse deviation from the off-momentum closed orbit. All the amplitude-dependent shift in transition gamma is contained in the first term of Eq. (3.7).

Now let us derive the additional path length difference due to space-charge tune shift. We obtain

$$-\frac{\Delta\ell_0}{2\pi} = \frac{\partial\Delta H}{\partial\delta} = \Delta N_{sc}(J_x, J_y) (-3 + 24\delta) - R [\Delta\alpha_{sc,0}\delta + \mathcal{O}(\delta^2)] . \quad (3.11)$$

The second term, which is amplitude independent, comes from the second term of Eq. (3.7) and $\Delta\alpha_{sc,0}$ is the lowest order modification to the momentum compaction. The first part of the first term on the right of Eq. (3.11) shows path length dependence on amplitude of a on-momentum particle, a reminisce of the terms fJ_x and gJ_y in the original equation of motion [Eq. (3.5)], and has its origin from the additional chromaticities

$$\Delta\xi_x = -3\Delta\nu_{sc,x}(1 - 8\delta), \quad \Delta\xi_y = -3\Delta\nu_{sc,y}(1 - 8\delta) . \quad (3.12)$$

The second part of the first term on the right side of Eq. (3.11) leads to amplitude-dependent momentum compaction. Comparing with the $d\delta^2$ term in Eq. (3.2) and remembering that $d = -\frac{1}{2}\alpha_0 R$, the self-field tune shift produces an up-shift in the momentum compaction ($\Delta\nu_{sc,0}$ is negative and $\Delta\alpha_{sc,0}$ is mostly positive)

$$\Delta\alpha_0 = -6\frac{\Delta N_{sc}}{R} + \Delta\alpha_{sc,0} , \quad (3.13)$$

or a down-shift of the transition gamma

$$\Delta\gamma_T = \gamma_T^3 \left(\frac{3\Delta N_{sc}}{R} - \frac{\Delta\alpha_{sc,0}}{2} \right) . \quad (3.14)$$

To have a better understanding, let us first assume the beam to be round and have a Kapchinskij-Vladimirskij (KV) distribution [7]. Then, the space-charge tune shift for all

[‡]Because of the same reason, besides what is contained in Eq. (3.7), there will not be any more alteration of the Hamiltonian of Eq. (3.2) by the space-charge tune shift. In particular, the terms $fJ_x\delta$ and $gJ_y\delta$ will not be changed; otherwise, the chromaticities exhibited in Eq. (3.6) will be altered.

beam particles with the same momentum offset and local longitudinal density will be the same and

$$\Delta N_{sc} = \Delta \nu_{sc}(J_x + J_y) , \quad (3.15)$$

where $\Delta \nu_{sc} = \Delta \nu_{sc,x} = \Delta \nu_{sc,y}$ and is given by Eq. (3.1) at the nominal momentum. We further assume the lattice to be FODO like so that Eq. (3.10) applies. Then the additional path length difference in Eq. (3.11) becomes

$$\frac{\Delta \ell_0}{C} = \Delta \nu_{sc}(3 - 12\delta) \frac{J_x + J_y}{R} - \left[\frac{2\Delta \nu_{sc}}{\gamma_T^3} \delta + \mathcal{O}(\delta^2) \right] , \quad (3.16)$$

where the last term is amplitude independent. Let us apply this to Phase II of the Fermilab Proton Driver, where the number per bunch is $N_b = 2.5 \times 10^{13}$ and rf harmonic $h = 18$. For the $\sigma_\tau = 1$ ns compressed bunch, the bucket bunching factor is $B_f \approx \sqrt{2\pi} h f_0 \sigma_\tau = 0.01899$. With normalized 95% emittance $\epsilon_{N95} = 60 \times 10^{-6}$ π m and an average betatron function of $\beta_x = 10$ m, the self-field space-charge tune shift is $\Delta \nu_{sc} = -0.297$. The maximum actions for betatron motion are only $J_x = J_y = 1.67 \times 10^{-6}$ m. The momentum aperture of the vacuum chamber is $\delta = 2\%$. With the nominal transition gamma of $\gamma_T = j27.71$, the maximum contributions to the additional fractional path difference are 2.62×10^{-8} for the first term of Eq. (3.16) and 5.57×10^{-7} for the second term. The maximum rf voltage used during the bunch rotation is $V_{rf} = 1.4$ MV, and the slip factor is $\eta = -0.00437$, giving a synchrotron tune of $\nu_s = 1.02 \times 10^{-3}$. Thus during the $\frac{1}{4}$ -synchrotron-period bunch rotation, the total cumulative maximum additional path difference due to space-charge tune shift is 0.32×10^{-6} for the first term and 4.56×10^{-5} for the second term. On the other hand, the ratio of the rms bunch length at extraction to the ring circumference is $\sigma_\tau/T_0 = 42.11 \times 10^{-5}$, which is much larger. These numbers are tabulated in Table III. Since the space-charge tune shift increases during the bunch rotation, a factor of $\frac{1}{2}$ was included in the computation of the first term of the cumulative path-length offset. Since the momentum spread also increases during the bunch rotation, a factor of $\frac{1}{3}$ was included in the computation of the second term. We also notice that the first term, which is amplitude dependent, is always an order of magnitude smaller than the second term. In conclusion, the effect of space-charge tune shift on bunch compression through rotation is very minimal for the present design of the Fermilab Proton Driver.

Next, let us relax the restriction of the KV distribution. Notice that in computing the contribution to $\Delta \ell_0/C$ of the particle with the largest J_x and J_y in Eq.(3.11), ΔN_{sc}

Table III: Fractional path-length offsets due to space-charge tune shift for the current design Phase II and an earlier design of the Fermilab Proton Driver. The cumulative fractional path-length offsets are found to be less than the bunch-length-to-ring-circumference ratio, σ_τ/T_0 , showing that the influence of space-charge tune shift is negligible for the bunch compression.

	Current Design Phase II	Earlier Design	
Circumference	711.32	180.65	m
Extraction kinetic energy	16	4.5	GeV
Number per bunch N_b	$2.5 \cdot 10^{13}$	$5.0 \cdot 10^{13}$	
95% normalized emittance ϵ_{N95}	$60 \cdot 10^{-6}$	$200 \cdot 10^{-6}$	πm
Betatron function β_x	10	10	m
Max. rf voltage V_{rf}	1.4	4.0	MV
Rf harmonic h	18	4	
Transition gamma γ_T	$j27.71$	$j10$	
Synchrotron tune ν_s	0.00102	0.00438	
<u>At extraction</u>			
Bunch length σ_τ	1	1	ns
Bunching factor B_f	0.0190	0.0164	
Space-charge tune shift ν_{sc}	-0.297	-0.450	
Max. betatron action J_x, J_y	$1.66 \cdot 10^{-6}$	$17.5 \cdot 10^{-6}$	m
Max. half momentum spread	0.02	0.02	
<u>Fractional path length offset per turn</u>			
First term of Eq. (3.16)	$0.26 \cdot 10^{-7}$	$0.16 \cdot 10^{-5}$	
Second term of Eq. (3.16)	$5.57 \cdot 10^{-7}$	$1.80 \cdot 10^{-5}$	
<u>Cumulative fractional path length offset for whole compression</u>			
First term of Eq. (3.16)	$0.32 \cdot 10^{-5}$	$0.47 \cdot 10^{-4}$	
Second term of Eq. (3.16)	$4.46 \cdot 10^{-5}$	$3.42 \cdot 10^{-4}$	
Bunch-length-to-ring-circum. ratio σ_τ/T_0	$42.1 \cdot 10^{-5}$	$16.6 \cdot 10^{-4}$	

is just the sum of the areas under the curves $\Delta\nu_{sc,x}$ as a function of J_x and $\Delta\nu_{sc,y}$ as a function of J_y . We have, on the other hand, $\Delta N_{sc} = \Delta\nu_{sc}(J_x + J_y)$ in the KV distribution. Thus, the computation of path length will follow exactly the example of the KV model if we substitute the KV space-charge tune shift $\Delta\nu_{sc}$ with $\langle\Delta\nu_{sc,x}\rangle$ and $\langle\Delta\nu_{sc,y}\rangle$, the mean value of the space-charge tune shifts over J_x or J_y . For a round beam with bi-Gaussian distribution truncated at 3 sigmas, $\langle\Delta\nu_{sc,x}\rangle$ or $\langle\Delta\nu_{sc,y}\rangle$ is approximately 1.65 times if the distribution were KV.

In the computation of the space-charge tune shift, for example $\Delta\nu_{sc,x}$, ϵ_{N95} in Eq. (3.1) should have been $\gamma\beta a_x^2/\beta_x$, where a_x is the horizontal radius of the beam that encloses 95% of the beam particle. However, in general,

$$a_x = \langle D \rangle \delta + \sqrt{2\beta_x J_x} , \quad (3.17)$$

where $\langle D \rangle$ is the average dispersion and has been so far neglected in our former discussion. For the present design of the Fermilab Proton Driver in Phase II, even if $\langle D \rangle \approx 1$ m, the dispersion contribution[§] at 2% momentum spread is $\langle D \rangle \delta = 20$ mm which is 3.5 larger than the maximum betatron contribution $\sqrt{2\beta_x J_x} = 5.77$ mm. In other words, the space-charge tune shift that goes into the path-length estimation in Eq. (3.16) should be an order of magnitude smaller. This will further diminish the influence of the space-charge tune shift.

Let us come back to the 4.5 GeV ring discussed earlier in this section. If the 95% normalized emittance is $\epsilon_{N95} = 400 \times 10^{-6}$ π m and the average betatron function is $\langle\beta_x\rangle \sim 10$ m, the space-charge tune shift is $\Delta\nu_{sc} = -0.450$ at extraction when the rms bunch length is compressed to $\sigma_\tau = 1$ ns. Near the end of the compression process, the fractional path-length offset per turn is 0.16×10^{-5} for the first term of Eq. (3.16) and 1.80×10^{-5} for the second term. With $V_{rf} = 4$ MV as the maximum rf voltage and $\gamma_T = j10$ as the transition gamma, the cumulative fractional path-length offset becomes 0.47×10^{-4} for the first term and 3.43×10^{-4} for the second. These are much smaller than the ratio of final bunch length to ring circumference $\sigma_\tau/T_0 = 16.6 \times 10^{-4}$. Again, the influence of space-charge tune shift is small. The results are tabulated in Table III.

On the other hand, the potential-well distortion due to space charge discussed in Sec. II

[§]A more accurate computation should take into account of the modification of horizontal dispersion and the introduction of vertical dispersion by the self-field space-charge tune shift. See Ref. [8] for detail.

can be more severe for this ring of the earlier design. For example, with a longitudinal space-charge impedance $|Z/n|_{\text{spch}} = 25 \Omega$ and a maximum rf voltage $V_{\text{rf}} = 4 \text{ MV}$, the space-charge-to-rf ratio is as large as 47.3.

There has been the idea of changing the lattice near extraction so that the beam is near transition and the bunch narrowing effect near transition can be utilized [9]. This does not appear to be an appealing idea. First, during the bunch compression, beam particles see a spread in space-charge tune shift $\Delta\nu_{sc}$ which translates into a spread in transition gamma of $\Delta\gamma_T \approx \Delta\nu_{sc}$ as a result of Umstatter effect. Thus, when the synchronous particle is less than $|\Delta\nu_{sc}|$ from the transition gamma, some particles will be above transition and some below making bunch rotation impossible, because some particles may be rotating clockwise and some counter-clockwise. Second, synchrotron oscillation will be slow when it is close to transition and a long duration will allow the growth of instabilities. Third, near transition higher order momentum compaction will be important. Space-charge tune shift introduces extra higher order momentum compaction which is dependent upon particle density, betatron amplitudes, as well as lattice structure. As a result, this contribution becomes a spread among the particles and it cannot be eliminated by sextupoles. Synchrotron motions of beam particles will therefore be very different depending on their momentum offset, betatron amplitude, and also location in the bunch, making bunch compression of an intense beam by rotation in the longitudinal phase space impossible.

It is important to point out that by having the $J_z\delta^2$ term in the additional Hamiltonian [Eq. (3.7)], we must include the same term into the original space-charge free Hamiltonian [Eq. (3.2)]. This term represents the next order chromaticity, which will contribute a down-shift to γ_T just like the first term Eq. (3.14) with $\Delta N_{sc} = \langle \Delta\nu_{sc,x} \rangle J_x + \langle \Delta\nu_{sc,y} \rangle J_y$ replaced by $\frac{1}{24}(\xi_{x1}J_x + \xi_{y1}J_y)$, where $\xi_z = \xi_{z0} + \xi_{z1}\delta + \dots$. For a linear machine, $\xi_{z1} = -2\xi_{z0}$. Thus, this order of chromaticity from the lattice can lead to a much larger spread in γ_T than the contribution from the space charge, and may require correction to ensure the bunch rotation.

IV CONCLUSION

We have discussed the longitudinal and transverse space-charge effects on the phase-space rotation of an intense proton bunch during bunch compression. The longitudinal space-charge force counteracts the rf focusing force. If the space-charge force is not too large, the slowing down of the synchrotron motion near the core of the bunch will help to cancel part of the linearity of the rf force. However, when the space-charge force is large enough, the bunch will be broadened during rotation so that bunch compression becomes impossible. Results of simulations and an experiment at the IUCF Cooler Ring indicate that the longitudinal space-charge effect will be negligible in Phase I (stage 2) of the Fermilab Proton Driver project. However, the space-charge force will be on the borderline in Phase II, where much shorter and more intense bunches are required.

Transversely, the space-charge force introduces incoherent betatron tune shifts during bunch rotation, which can be even larger than the self-field tune shifts at injection. It is possible that particles with different betatron tunes will have different path lengths and will therefore jeopardize the bunch rotation process. The most important contribution to path length difference is Umstätter effect which has momentum spread dependency. The less important contribution is betatron amplitude dependency. It has been found that the largest cumulative fractional path length offset during the whole bunch rotation is still one order of magnitude less than the ratio of the compressed rms bunch length and the ring circumference in the current design of the Fermilab Proton Driver in Phase II. Thus it can be concluded that the influence of space-charge tune shift on bunch compression is negligibly small unless the transition energy of the ring is very close to the extraction energy of the ring, at which the bunch rotation is performed. On the other hand, the chromaticities of the accelerator ring may have a much larger modification of the amplitude-dependent momentum compaction and therefore much larger contribution to the path length difference. Chromaticity correction of the lowest order and possibly also the next order may be necessary to ensure the bunch rotation.

Finally, we have given, in the Appendices, deeper insight into the relation between path length increase due to finite betatron oscillation amplitudes and chromaticity correction. In the presence of sextupoles, it has been shown explicitly that chromaticity correction does indeed shorten the particle path length.

ACKNOWLEDGMENT

The author wishes to thank Dr. Sho Ohnuma for many stimulating discussions.

APPENDIX

A CANONICAL VARIABLES

In the Frenet-Serret coordinate system, the canonical pairs are

$$(z, p_z) \quad \text{and} \quad (-\Delta t, \Delta E) , \quad (\text{A.1})$$

where $z = x$ or y , ΔE is the energy offset of the particle from the design energy of the ring, and Δt is average extra time taken by the particle to complete a revolution. Using the generating function

$$F_2(\Delta t, \Delta p) = -\Delta t \left[\sqrt{(\Delta p + p_0)^2 + m^2 c^4} - E_0 \right] , \quad (\text{A.2})$$

where p_0 and E_0 are the design *total* momentum and energy of the ring and Δp the momentum offset of the particle with rest mass m , $(-\Delta t, \Delta E)$ is transformed to $(-\Delta \ell, \Delta p)$, where

$$\begin{cases} \Delta E = \frac{\partial F_2}{\partial(-t)} = \sqrt{(\Delta p + p_0)^2 + m^2 c^4} - E_0 = E - E_0 , \\ -\Delta \ell = \frac{\partial F_2}{\partial \Delta p} = -v \Delta t . \end{cases} \quad (\text{A.3})$$

Thus $\Delta \ell$ is the path length offset per turn with v the particle velocity. The Frenet-Serret Hamiltonian is p_s , the longitudinal momentum. Performing a scale transformation so that the new Hamiltonian is p_s/p_0 , the canonical coordinate pairs become

$$(z, z') \quad \text{and} \quad (-\Delta \ell, \delta) , \quad (\text{A.4})$$

where $z' = p_z/p_0$ and $\delta = \Delta p/p_0$.

B PATH LENGTH AND CHROMATICITIES

In order to better understand why the particle path length can be independent of betatron amplitudes, we try to compute the actual path length. The path length of a particle is given by

$$C = \sqrt{\left(1 + \frac{x}{\rho}\right)^2 + x'^2 + y'^2} , \quad (\text{B.5})$$

where prime denotes the derivative with respect to the distance s along the design closed orbit and ρ is the radius of curvature at s . If we do an expansion and keep up to the second order terms, we have for the relative path difference,

$$\frac{\Delta C}{C_0} = \frac{x}{\rho} + \frac{x'^2}{2} + \frac{y'^2}{2} , \quad (\text{B.6})$$

where the x^2/ρ^2 terms just cancel each other. First consider a linear lattice with only dipoles and normal quadrupoles. Let us consider only on-momentum particles. The horizontal and vertical motions can be written as

$$x = \sqrt{2\beta_x J_x} \cos(\psi_x + \varphi_x) , \quad (\text{B.7})$$

$$y = \sqrt{2\beta_y J_y} \cos(\psi_y + \varphi_y) , \quad (\text{B.8})$$

where

$$\psi_x(s) = \int^s \frac{ds'}{\beta_x(s')} \quad \text{and} \quad \psi_y(s) = \int^s \frac{ds'}{\beta_y(s')} \quad (\text{B.9})$$

are the horizontal and vertical Floquet phase advances. To take care of the fact that the particle passes through location s at different x and y every turn, we have introduced the random phases φ_x and φ_y . It is clear that x/ρ does not contribute in a linear machine when averaged over φ_x . It is easy to compute

$$\begin{aligned} x' &= -\sqrt{\frac{2J_x}{\beta_x}} \left[\sin(\psi_x + \varphi_x) + \alpha_x \cos(\psi_x + \varphi_x) \right] , \\ y' &= -\sqrt{\frac{2J_y}{\beta_y}} \left[\sin(\psi_y + \varphi_y) + \alpha_y \cos(\psi_y + \varphi_y) \right] , \end{aligned} \quad (\text{B.10})$$

where $\alpha_x = -\frac{1}{2}\beta'_x$ and $\alpha_y = -\frac{1}{2}\beta'_y$, with the prime denoting derivative with respect to s . Hence, we obtain

$$\frac{\Delta C}{C_0} = \frac{J_x}{2} \left\langle \frac{1 + \alpha_x^2}{\beta_x} \right\rangle + \frac{J_y}{2} \left\langle \frac{1 + \alpha_y^2}{\beta_y} \right\rangle . \quad (\text{B.11})$$

Thus, from Eq. (3.5), we can identify

$$f = -\frac{R}{2} \left\langle \frac{1 + \alpha_x^2}{\beta_x} \right\rangle \quad \text{and} \quad g = -\frac{R}{2} \left\langle \frac{1 + \alpha_y^2}{\beta_y} \right\rangle . \quad (\text{B.12})$$

On the other hand, the natural chromaticities are

$$\xi_z = -\frac{1}{4\pi} \oint \beta_z(s) K_z(s) ds \quad z = x, y , \quad (\text{B.13})$$

where the focusing strengths[¶]

$$K_x(s) = \frac{1}{\rho^2(s)} + \frac{B'_y(s)}{(B\rho)_0} \quad \text{and} \quad K_y(s) = -\frac{B'_y(s)}{(B\rho)_0}, \quad (\text{B.14})$$

with B'_y being the quadrupole gradient (derivative with respect to x) and $(B\rho)_0$ the magnetic rigidity of the on-momentum particle, are related to the Twiss parameters by

$$K_z\beta_z = \alpha'_z + \frac{1 + \alpha_z^2}{\beta_z} \quad z = x, y. \quad (\text{B.15})$$

It is then easy to show that

$$\xi_z = -\frac{R}{2} \left\langle \frac{1 + \alpha_z^2}{\beta_z} \right\rangle \quad z = x, y, \quad (\text{B.16})$$

which are exactly f and g given in Eq. (B.12).

C SEXTUPOLES AND PATH LENGTH COMPENSATION

Now let us put in sextupoles that correct for the chromaticities and investigate how the particle path length becomes shortened. Betatron oscillations with finite amplitudes will contribute positively to x'^2 and y'^2 . Thus, according to Eq. (B.5) or (B.6), it appears to be difficult to understand how the path length can be compensated by chromaticity correction. The answer lies in the fact that the closed orbit with finite betatron amplitudes moves inward and is therefore shortened. The magnetic field pattern of an F -sextupole correcting for the horizontal chromaticity is shown in Fig. 8(a), where the particle motion is coming out of the paper. Here, the dispersion function at the sextupole is assumed positive. The directions of the magnetic field are correct because a particle with positive momentum offset will most probably cross the sextupole near the large dot with $x > 0$, see a positive vertical magnetic field B_y , and receive a kick with $x' < 0$, or towards the center of the accelerator ring, thus enhancing the F -quadrupole focusing. On the other, a

[¶]Here, (x, y, s) forms a right-handed coordinate system, where x represents the horizontal displacement, y represents the vertical displacement, and s is the direction of the beam longitudinal motion. This implies that $B'_y = dB_y/dx > 0$ for the F -quadrupole and $B'_y < 0$ for the D -quadrupole.

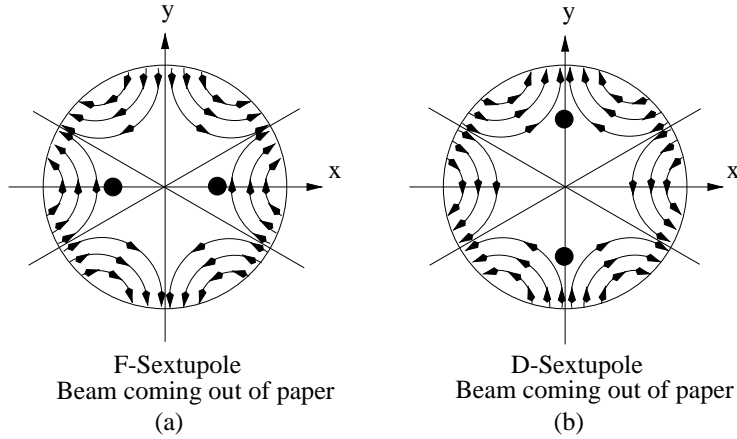


Figure 8: Magnetic field pattern of (a) an F -sextupole correcting for the horizontal chromaticity and (b) a D -sextupole correcting for the vertical chromaticity, with the direction of particle motion coming out of the figure. Notice that a particle with horizontal betatron displacement crossing the F -sextupole or vertical betatron displacement crossing the D -sextupole will see a positive vertical magnet field and will therefore be kicked towards the center of the ring. Here, the dispersion function at the sextupoles has been assumed to be positive.

particle with negative momentum offset will most probably cross the sextupole near the large dot with $x < 0$, see a positive vertical magnetic field B_y , and receive a kick with $x' < 0$, or towards the center of the accelerator ring, thus weakening the F -quadrupole focusing.

Now consider an on-momentum particle with a finite betatron oscillation amplitude. It is clear that particle crossing the sextupole with a horizontal displacement like either large dots in the figure (the average vertical displacement should be much smaller because $\beta_x \gg \beta_y$ at the F -sextupole) will receive a kick with $x' < 0$, or towards the center of the accelerator ring, independent of whether the horizontal displacement is positive or negative. The same is true for a D -sextupole, whose magnetic field is depicted in Fig. 8(b). A particle crossing the sextupole with a vertical displacement like the large dots in the figure will see a positive vertical magnetic field B_y and receive a kick with $x' < 0$ as well. Thus chromaticity correction sextupoles will move the averaged closed orbit of particles with betatron amplitudes inside the designed closed orbit (with zero betatron amplitudes). An inner orbit has shorter path length, therefore compensating for the extra excursion of the betatron oscillations. The contribution of the sextupoles

must come from the x/ρ term in Eq. (B.5) or (B.6). Thus, the contribution becomes global and is derived from the dipoles where the radius of curvature is nonzero. This is understandable, because dipoles generate dispersion, from which the sextupoles are able to correct for the chromaticities. The effect is global because the ring is a closed entity. In below, we are going to show that this global contribution sums up to exactly the chromaticity corrections. As an illustration, we introduce a lattice consisting of 14 FODO cells plus some long straight sections. Each cell has horizontal and vertical phase advances 90.0° and 85.8° . The quadrupoles are thin and between them are filled with dipoles. As shown in Fig. 9 is the design closed orbit AB for two FODO cells starting from a half F -quadrupole and ending with a half F -quadrupole. The radius of curvature at the dipoles is 30 units. A particle starting at A with a horizontal offset x but zero x' is tracked for two FODO cells. The path is shown in dashes when all sextupoles are turned

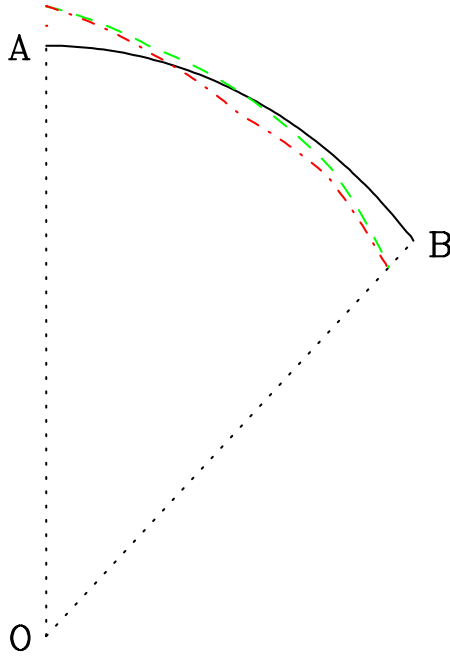


Figure 9: (color) A particle is tracked for two FODO cells AB each having horizontal and vertical phase advances 90.0° and 85.8° . The starting and ending elements are both half F -quadrupoles. With an initial horizontal offset x but zero x' , its path is shown as dashes when all the sextupoles are off, and becomes dot-dashed when the sextupoles canceling chromaticities are on. It is evident that the path length becomes shorter with the chromaticities corrected.

off. All the sextupoles at the F and D quadrupoles are now turned on so that both the horizontal and vertical chromaticities are canceled. The particle is tracked again and its path is shown as dot-dashed. It is evident that the path length becomes shorter than when the sextupoles are turned off.

Because sextupoles bring about nonlinearity to the lattice, the horizontal displacement of the particle is no longer given by the linear term $\mathcal{O}(\sqrt{J_x})$ in Eq. (B.7), which averages to zero over the random phase φ_x . In fact, there is a $\mathcal{O}(J_x)$ term which does not vanish when averaged over the random phase φ_x and must be included in the x/ρ term. It is the closed orbit distortion $\delta x(s)$ due to presence of the sextupoles and is given by [10, 12, 13]

$$\delta x(s) = 2\sqrt{\beta_x} \left[-2J_x B_1(\psi_x) + 2J_y \bar{B}(\psi_x) \right]. \quad (\text{C.1})$$

In above, $B_1(\psi_x)$ and $\bar{B}(\psi_x)$ are two of the 5 *distortion functions* introduced by Tom Collins to describe the orbit distortion in the presence of the sextupoles. They have the following properties: [10, 12, 11, 13]

1. They are periodic functions of the ring.
2. (B_1, B'_1) and (\bar{B}, \bar{B}') , where the prime represents derivative with respect to ψ_x , rotate like vectors by the Floquet angle ψ_x along the ring when there is no sextupole.
3. On crossing the k -th thin sextupole of length ℓ at location s_k , B_1 and \bar{B} are continuous, while B'_1 and \bar{B}' jump, respectively, by $\frac{1}{4}S_k$ and $\frac{1}{4}\bar{S}_k$, where

$$S_k = \lim_{\ell \rightarrow 0} \left[\beta_x^{3/2} \frac{B_y'' \ell}{2(B\rho)_0} \right]_k \quad \text{and} \quad \bar{S}_k = \lim_{\ell \rightarrow 0} \left[\beta_x^{1/2} \beta_y \frac{B_y'' \ell}{2(B\rho)_0} \right]_k, \quad (\text{C.2})$$

with $(B_y'' \ell)_k$ representing the integrated strength of the k -th sextupole.

From these 3 properties, B_1 and \bar{B} can be written explicitly as

$$B_1(\psi_x) = \frac{1}{2 \sin \pi \nu_x} \sum_k \frac{S_k}{4} \cos \left(|\psi_x - \psi_{xk}| - \pi \nu_x \right), \quad (\text{C.3})$$

$$\bar{B}(\psi_x) = \frac{1}{2 \sin \pi \nu_x} \sum_k \frac{\bar{S}_k}{4} \cos \left(|\psi_x - \psi_{xk}| - \pi \nu_x \right), \quad (\text{C.4})$$

where the summation is over all the sextupoles in the ring.

We next make use of the fact the dispersion D satisfies

$$\frac{d^2 D}{ds^2} + K_x D = \frac{1}{\rho} \quad (\text{C.5})$$

to arrive at

$$\oint \frac{\delta x}{\rho} ds \Rightarrow -\frac{J_x}{2 \sin \pi \nu_x} \sum_k S_k \oint \hat{x} \left(\frac{d^2 D}{ds^2} + K_x D \right) ds, \quad (\text{C.6})$$

where we have dropped the J_y -term for the time being and used the short-hand notation

$$\hat{x} = \sqrt{\beta_x} \cos \left(|\psi_x - \psi_{xk}| - \pi \nu_x \right). \quad (\text{C.7})$$

Notice that away from sextupoles, \hat{x} satisfies the homogeneous Hill's equation

$$\frac{d^2 \hat{x}}{ds^2} + K_x \hat{x} = 0. \quad (\text{C.8})$$

Thus, we can integrate Eq. (C.7) by parts to get

$$\oint \frac{\delta x}{\rho} ds \Rightarrow \frac{J_x}{2 \sin \pi \nu_x} \sum_k S_k \left[D \frac{d\hat{x}}{ds} \right]_{s_k+}^{s_k-} = -J_x \sum_k \left[\frac{SD}{\sqrt{\beta_x}} \right]_k, \quad (\text{C.9})$$

where across the k -th sextupole, the integration has been performed to s_k- just before the sextupole and from s_k+ just after the sextupole. Also use has been made of the fact that \hat{x} is continuous across the k -th sextupole while $\frac{d\hat{x}}{ds}$ jumps by $\frac{2 \sin \pi \nu_x}{\sqrt{\beta_{xk}}}$. Including the J_y -term and using Eq. (C.2), we finally obtain

$$\oint \frac{\delta x}{\rho} ds = -J_x \sum_k \left[\beta_x D \frac{B_y'' \ell}{2(B\rho)_0} \right]_k + J_y \sum_k \left[\beta_y D \frac{B_y'' \ell}{2(B\rho)_0} \right]_k. \quad (\text{C.10})$$

Since $DB_y'' \ell$ is positive for the F -sextupoles and negative for the D -sextupoles, the path length of the averaged closed orbit is indeed reduced in the presence of finite betatron amplitudes. The chromaticity corrections by the sextupoles are

$$\Delta \xi_x = \frac{1}{4\pi} \sum_k \left[\beta_x D \frac{B_y'' \ell}{(B\rho)_0} \right]_k \quad \text{and} \quad \Delta \xi_y = -\frac{1}{4\pi} \sum_k \left[\beta_y D \frac{B_y'' \ell}{(B\rho)_0} \right]_k, \quad (\text{C.11})$$

which are both positive for natural chromaticity compensation. Notice that we have not included the sextupole contribution to x'^2 and y'^2 in Eq. (B.5). This is because so far we

have been working up to first order in sextupole strength. Complementary to Eq. (C.1), the sextupole modification of the closed orbit is also given by

$$\delta x'(s) = 2\sqrt{\beta_x} \left[-2J_x B_1'(\psi_x) + 2J_y \bar{B}'(\psi_x) \right], \quad (\text{C.12})$$

which, together with Eq. (B.10), gives the horizontal divergence of the particle. In computing x'^2 , the cross term vanishes when averaged over the random phase φ_x . Thus the sextupole contribution is second order in the sextupole strength.

Including the linear part of the lattice, we can therefore write

$$\Delta C = 2\pi J_x \left[\frac{R}{2} \left\langle \frac{1 + \alpha_x^2}{\beta_x} \right\rangle - \Delta \xi_x \right] + 2\pi J_y \left[\frac{R}{2} \left\langle \frac{1 + \alpha_y^2}{\beta_y} \right\rangle - \Delta \xi_y \right], \quad (\text{C.13})$$

or^{||}

$$\Delta C = -2\pi \left[J_x (\xi_x + \Delta \xi_x) + J_y (\xi_y + \Delta \xi_y) \right], \quad (\text{C.14})$$

where ξ_x and ξ_y are the horizontal and vertical natural chromaticities. The reduction of the orbit length enhancement due to finite betatron amplitudes by chromaticity correction now becomes obvious.

The contribution from other nonlinear elements in the lattice can be computed in a similar way when the concept of distortion functions is extended [14].

^{||}The result in Eq.(C.14) has also been quoted in Ref. [5]. However, no derivation has been given.

References

- [1] K.M. Fung, M. Ball, C.M. Chu, B. Hamilton, S.Y. Lee, and K.Y. Ng, Phys. Rev. ST Accel. Beams **3**, 100101 (2000).
- [2] The $\mu^+\mu^-$ Collider Collaboration, *Muon Muon Collider: Feasibility Study*, BNL Report BNL-52503, Fermilab Report Conf-96/092, LBL Report LBNL-38946, 1996.
- [3] R.B. Palmer, talk given at the 9th Advanced ICFA Beam Dynamics Workshop on Beam Dynamics and Technology Issues for $\mu^+\mu^-$ Colliders, Montauk, NY, Oct. 15-20, 1995.
- [4] K.Y. Ng, *Beam Stability Issues in a Quasi-Isochronous Muon Collider*, Proceedings of the 9th Advanced ICFA Beam Dynamics Workshop on Beam Dynamics and Technology Issues for $\mu^+\mu^-$ Colliders, Montauk, NY, Oct. 15-20, 1995, Ed. J.C. Gallardo, p.224.
- [5] L. Emery, *Coupling of Betatron Motion to the Longitudinal Plane Through Path Lengthening in Low- α_c Storage Rings*, Proceedings of the XVth International Conference on High Energy Accelerators, Hamburg, July 20-24, 1992, Ed. J. Rossbach, p.1172.
- [6] E. Forest, private communication.
- [7] I.M. Kapchinskij and V.V. Vladimirskij, Proc. 2nd Int. Conf. High Energy Accel. and Instr., CERN, Geneva, 1959, p. 274.
- [8] S.Y. Lee and H. Okamoto, Phys. Rev. Lett. **23**, 5133 (1998).
- [9] C. Ankenbrandt, et al., Phys. Rev. ST Accel. Beams **1**, 030101 (1999).
- [10] T.L. Collins, *Distortion Functions*, Fermilab Internal Report 84/114 (1984).
- [11] K.Y. Ng, *Comparison of the Second-Order Tune Shift Formulas due to Sextupoles given by Collins and Ohnuma*, Proceedings of the 1984 Summer Study on the Design and Utilization of the Superconducting Super Collider, Snowmass, Colorado, 1984.
- [12] K.Y. Ng, *Derivation of Collins' Formulas for Beam-Shape Distortion due to Sextupoles using Hamiltonian Method*, Fermilab Report TM-1281 (1984).

- [13] K.Y. Ng, *Distortion Functions*, KEK Report 87-11 (1987) or Fermilab Report FN-455 (1987).
- [14] L. Merminga and K.Y. Ng, *Hamiltonian Approach to Distortion Functions*, Fermilab Report FN-493 (1988), revised (1992).